LBL-30296
Preprint

Lawrence Berkeley Laboratory
UNIVERSITY OF CALIFORNIA

Submitted to Physical Review C

Neutron and Hybrid Stars in the Derivative Coupling Model

N.K. Glendenning, F. Weber, and S.A. Moszkowski

May 1991

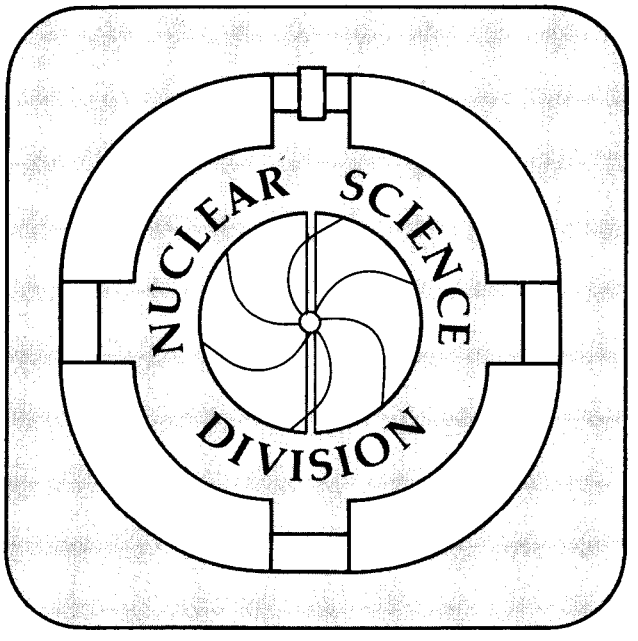

LBL-30296
Copy 2
| LOAN COPY |
|Circulates |
|for 4 weeks| Bldg. 50 Library.

Prepared for the U.S. Department of Energy under Contract Number DE-AC03-76SF00098

DISCLAIMER

This document was prepared as an account of work sponsored by the United States Government. While this document is believed to contain correct information, neither the United States Government nor any agency thereof, nor the Regents of the University of California, nor any of their employees, makes any warranty, express or implied, or assumes any legal responsibility for the accuracy, completeness, or usefulness of any information, apparatus, product, or process disclosed, or represents that its use would not infringe privately owned rights. Reference herein to any specific commercial product, process, or service by its trade name, trademark, manufacturer, or otherwise, does not necessarily constitute or imply its endorsement, recommendation, or favoring by the United States Government or any agency thereof, or the Regents of the University of California. The views and opinions of authors expressed herein do not necessarily state or reflect those of the United States Government or any agency thereof or the Regents of the University of California.

LBL-30296

Neutron and Hybrid Stars in the Derivative Coupling Model†

N. K. Glendenning, F. Weber‡

Nuclear Science Division
Lawrence Berkeley Laboratory
University of California
One Cyclotron Road
Berkeley, California 94720

S. A. Moszkowski

University of California at Los Angeles
Department of Physics
Los Angeles, California 90024

May 1, 1991

PACS 21.65+f 21.80.+a 97.60.Jd 95.30.Cq 12.38.Mh

†This work was supported by the Director, Office of Energy Research, Office of High Energy and Nuclear Physics, Division of Nuclear Physics, of the U.S. Department of Energy under Contract DE-AC03-76SF00098.

‡Supported by a fellowship from the Max Kade Foundation.

Neutron and Hybrid Stars in the Derivative Coupling Model†

N. K. Glendenning, F. Weber‡

Nuclear Science Division
Lawrence Berkeley Laboratory
University of California
One Cyclotron Road
Berkeley, California 94720

S. A. Moszkowski

University of California at Los Angeles
Department of Physics
Los Angeles, California 90024

May 1, 1991

ABSTRACT

Properties of neutron stars derived from the hybrid derivative coupling model of nuclear field theory are studied. Generalized beta equilibrium with all baryon types to convergence is allowed. Hyperon couplings compatible with the inferred binding energy of the lambda hyperon in saturated nuclear matter are used. Among the properties studied are the limits on rotation imposed by gravitation-radiation reaction instabilities as moderated by viscosity. Consistent with our other investigations, these instabilities place a lower limit on rotational periods of neutron and hybrid stars of about 1 ms. The possible transition of the core to quark matter was considered. This is a first order phase transition with two conserved charges, baryon and electric. Consequently, the pressure varies as the concentration in the mixed phase so that the presence of the mixed phase in the core can extend over a finite radial extension, unlike the phase transition of a substance having only one conserved charge. For a reasonable bag model equation of state for quark matter we find that the hadronic matter in the star begins its conversion to quark matter at about three times nuclear density and that the entire core of the star is in the mixed phase.

†This work was supported by the Director, Office of Energy Research, Office of High Energy and Nuclear Physics, Division of Nuclear Physics, of the U.S. Department of Energy under Contract DE-AC03-76SF00098.

‡Supported by a fellowship from the Max Kade Foundation.

Contents

1 Introduction **1**

2 Hybrid Derivative Coupling Nuclear Field Theory **2**

3 Neutron Star Structure **7**

3.1 Baryon Populations 7

3.2 Hyperon Couplings: Constraints from Hyperon Binding in Nuclei . . 8

3.3 Mass-Radius Relation, Kepler Frequency, Moment of Inertia 10

4 Hybrid Quark-Neutron Star **12**

5 Gravitational Radiation-Reaction Instability **17**

6 Summary **19**

Neutron and Hybrid Stars in the Derivative Coupling Model

N. K. Glendenning, F. Weber and S. A. Moszkowski

1 Introduction

Relativistic field theories of nuclear matter and finite nuclei have enjoyed a renaissance in recent years, not because most nuclear properties cannot be accounted for in the Schroedinger approach, but because we know that nuclear forces arise from the exchange of mesons (or at a more basic level, quarks), and the presence of meson currents in nuclei is well established [1]. In certain cases relativistic theory provides a better description than the non-relativistic Schroedinger [2, 3]. Moreover, in seeking a description of high density hadronic matter, a covariant theory has the advantage of automatically respecting causality, which Schroedinger based theories ultimately violate.

The $\sigma - \omega$ nuclear field theory has been broadly studied both in spherical and deformed nuclei. However in the linear version [4] it has too small a nucleon effective mass ($\sim .55 m_N$) at saturation density of nuclear matter, and too large a compression modulus ($\sim$ 560 MeV). These properties can be brought under control at the cost of two additional parameters by the addition of scalar cubic and quartic self-interactions in the so-called non-linear model [5]. Alternately it has been recently noticed by Zimanyi and Moszkowski [6] that if the scalar field is coupled to the derivative of the nucleon field, these two nuclear properties are automatically in fairly reasonable accord with present knowledge of their values, the two coupling constants of the theory being fixed by the empirical saturation density and binding as in the linear $\sigma - \omega$ theory. The agreement with bulk nuclear properties can be further improved by a slight modification of the model of Zimanyi and Moszkowski, which we shall call the hybrid derivative coupling model, and which we discuss below. Renormalization is irrevocably lost in derivative coupling models but since (strong interacting) nuclear field theory is usually regarded as an effective one, this does not seem to be a weighty objection. Since in the derivative coupling model only two coupling constants are needed to reproduce four nuclear properties ($\rho_0, B/A, m^\star, K$), the last two albeit approximately, it is interesting to explore its predictions for neutron star properties. This we do for a wider range of properties than is usual. For example we calculate the general relativisitic Kepler frequency for the family of stars, the gravity wave instabilities as moderated by viscosity, and the conversion of the core of the heavier

neutron stars to the mixed phase of hadronic and quark matter, properly taking into account the modifications introduced into first order phase transitions in systems possessing more than one conserved charge, as is necessarily the case for neutron stars. In addition we discuss the connection of the Lambda hyperon binding as inferred from measurements of energy levels in hypernuclei, and the coupling constants of the theory. We find, unlike earlier works [7, 8, 9], that the coupling in the two systems, hypernuclei and neutron stars, *can* be reconciled.

Neutron stars are not pure in neutrons, as their name might imply. The lowest energy state of cold, charge neutral matter is not pure neutron matter, but matter that is in beta equilibrium. At the high densities that may be present in the cores of the most massive neutron stars, this equilibrium will involve not only the neutron, proton and leptons, but also such higher mass baryons for which the baryon chemical potential exceeds their mass (corrected for interactions and electric charge). We need therefore to generalize the Lagrangian for nuclear matter analogous to the way the earlier theories were generalized [10, 11].

2 Hybrid Derivative Coupling Nuclear Field Theory

In place of the purely derivative coupling of the scalar field to the baryons and vector meson of the Zimanyi-Moszkowski model, we here couple it by both Yukawa point and derivative coupling to baryons and both vector fields. This improves the agreement with the compression modulus and effective nucleon mass at saturation. The nuclear matter properties are quoted later. To account for the symmetry force we include the coupling of the rho meson to the isospin current. (The rho meson contribution to this current vanishes in the mean field approximation and so we do not write its formal contribution in the Lagrangian [12].)

$$\begin{aligned}
\mathcal{L} \;=\; & \sum_B \Big[\Big(1+\frac{g_{\sigma B}\,\sigma}{2m_B}\Big)\Big\{\overline{\psi}_B[i\gamma_\mu\partial^\mu - g_{\omega B}\gamma_\mu\omega^\mu - \tfrac{1}{2}g_{\rho B}\gamma_\mu\boldsymbol{\tau}\cdot\boldsymbol{\rho}^\mu]\psi_B\Big\} \\
& -\Big(1-\frac{g_{\sigma B}\,\sigma}{2m_B}\Big)m_B\overline{\psi}_B\psi_B\Big] \\
& + \tfrac{1}{2}(\partial_\mu\sigma\partial^\mu\sigma - m_\sigma^2\sigma^2) - \tfrac{1}{4}\omega_{\mu\nu}\omega^{\mu\nu} + \tfrac{1}{2}m_\omega^2\omega_\mu\omega^\mu \\
& - \tfrac{1}{4}\boldsymbol{\rho}_{\mu\nu}\cdot\boldsymbol{\rho}^{\mu\nu} + \tfrac{1}{2}m_\rho^2\boldsymbol{\rho}_\mu\cdot\boldsymbol{\rho}^\mu + \sum_\lambda \overline{\psi}_\lambda(i\gamma_\mu\partial^\mu - m_\lambda)\psi_\lambda. \qquad (1)
\end{aligned}$$

In the first line one sees the coupling of the scalar field to the derivatives of the baryon fields and to the vector mesons. The Yukawa point coupling to the baryon fields is contained in the second line. In the last two lines one recognizes the free scalar, vector, vector-isovector mesons and lepton Lagrangians. The latter must be present because of charge neutrality. (We use the notation $\omega_{\mu\nu} = \partial_\mu\omega_\nu - \partial_\nu\omega_\mu$ and other conventions of ref. [13].) The baryon Lagrangian is in the first line together with the interaction terms with the above mentioned mesons. The ρ-meson coupling constant will be adjusted to give the empirical symmetry coefficient. The sum on B

is extended over all baryons *including their charge states* to convergence, of which the most obvious are listed in Table 1. The solution is most easily obtained by means of the transformation of all baryon fields by,

$$\psi_B = \left(1 + \frac{g_{\sigma B}\,\sigma}{2m_B}\right)^{-1/2} \Psi_B. \tag{2}$$

The equivalent Lagrangian is

$$\begin{aligned}
\mathcal{L} &= \sum_B \overline{\Psi}_B[i\gamma_\mu\partial^\mu - m_B^\star - g_{\omega B}\gamma_\mu\omega^\mu - \tfrac{1}{2}g_{\rho B}\gamma_\mu\boldsymbol{\tau}\cdot\boldsymbol{\rho}^\mu]\Psi_B \\
&\quad + \tfrac{1}{2}(\partial_\mu\sigma\partial^\mu\sigma - m_\sigma^2\sigma^2) - \tfrac{1}{4}\omega_{\mu\nu}\omega^{\mu\nu} + \tfrac{1}{2}m_\omega^2\omega_\mu\omega^\mu \\
&\quad - \tfrac{1}{4}\boldsymbol{\rho}_{\mu\nu}\cdot\boldsymbol{\rho}^{\mu\nu} + \tfrac{1}{2}m_\rho^2\boldsymbol{\rho}_\mu\cdot\boldsymbol{\rho}^\mu + \sum_\lambda \overline{\psi}_\lambda(i\gamma_\mu\partial^\mu - m_\lambda)\psi_\lambda.
\end{aligned} \tag{3}$$

It is evident that the baryons now have effective masses,

$$m_B^\star = \left(1 - \frac{g_{\sigma B}\,\sigma}{2m_B}\right)\left(1 + \frac{g_{\sigma B}\,\sigma}{2m_B}\right)^{-1} m_B. \tag{4}$$

We solve the Euler-Lagrange equations following from this Lagrangian in the mean field approximation by replacing the baryon source currents in the meson equations by their ground state expectation values. The ground state is defined as having the single-particle momentum eigenstates of the Dirac equations filled to the top of the Fermi sea for each baryon species in accord with the conditions of chemical equilibrium. We describe how this is done below.

The meson field equations in uniform static matter, in which space and time derivatives can be dropped, are,

$$\omega_0 = \sum_B \frac{g_{\omega B}}{m_\omega^2} n_B \tag{5}$$

$$\rho_{03} = \sum_B \frac{g_{\rho B}}{m_\rho^2} I_{3B} n_B \tag{6}$$

$$\begin{aligned}
m_\sigma^2\sigma &= \sum_B g_{\sigma B}\left(1 + \frac{g_{\sigma B}\,\sigma}{2m_B}\right)^{-2} \langle\overline{\Psi}_B\Psi_B\rangle \\
&= \sum_B g_{\sigma B}\left(1 + \frac{g_{\sigma B}\,\sigma}{2m_B}\right)^{-2} \frac{2J_B+1}{2\pi^2}\int_0^{k_B} \frac{m_B^\star}{\sqrt{k^2 + m_B^{\star\,2}}}\,k^2\,dk.
\end{aligned} \tag{7}$$

The bracket, $\langle\cdots\rangle$ denotes ground state expectation. A simple way of computing such expectation values without the need of constructing the Dirac spinors is described in ref.[11]. The space-like components of both vector fields vanish as can be shown explicitly [11]; they do so for the physical reasons that the ground state is isotropic and has definite charge.

The condition of charge neutrality is expressed by,

$$\begin{aligned}
q_H + q_e &= 0, \\
q_H &\equiv \sum_B (2J_B+1)q_B k_B^3/(6\pi^2), \qquad q_e \equiv -\sum_\lambda k_\lambda^3/(3\pi^2) = 0,
\end{aligned} \tag{8}$$

where the first sum is over the baryons whose electric charges are denoted by q_B, Fermi momenta by k_B and the second sum is over the leptons e^- and μ^-.

Chemical equilibrium can be imposed through the two independent chemical potentials, μ_n, μ_e, for the conserved baryon and (negative) electron charge. Strangeness is not conserved on any macroscopic time scale. For the baryon species, B, we have $\mu_B = \mu_n - q_B\mu_e$. The Fermi momenta for the baryons are the positive real solutions of

$$\mu_B = e_B(k_B), \qquad \text{(N equations)} \tag{9}$$

where N is the number of different baryon species including their charge states that are listed in Table 1, and the Dirac eigenvalues, $e_B(k)$ are defined below. The lepton Fermi momenta are the positive real solutions of,

$$\sqrt{k_e^2 + m_e^2} = \mu_e \tag{10}$$

$$\sqrt{k_\mu^2 + m_\mu^2} = \mu_\mu = \mu_e. \tag{11}$$

At a chosen baryon density

$$\rho = \sum_B n_B \tag{12}$$

$$n_B \equiv \langle \Psi_B^\dagger \Psi_B \rangle = (2J_B + 1)k_B^3/(6\pi^2), \tag{13}$$

the solution of the above coupled equations (5-12) provides the values for

$$\sigma, \omega_0, \rho_{03}, \mu_n, \mu_e, k_e, k_\mu, k_n, k_p, k_\Lambda ..... \tag{14}$$

of which there are (7+N).

The Dirac equations for the baryons are,

$$(i\gamma_\mu \partial^\mu - m_B^\star - g_{\omega B}\gamma_\mu \omega^\mu - \tfrac{1}{2} g_{\rho B}\gamma_\mu \boldsymbol{\tau} \cdot \boldsymbol{\rho}^\mu)\Psi_B = 0. \tag{15}$$

Taking account of the vanishing of the space-like components of the vector fields the eigenvalues can be found as,

$$e_B(k) = g_{\omega B}\omega_0 + g_{\rho B}\rho_{03} I_{3B} + \sqrt{k^2 + m_B^{\star\,2}}. \tag{16}$$

In the above equations, I_{3B} is the isospin projection of baryon charge state B. This completes a description of the equations that define the solution of the above Lagrangian for charge neutral matter in equilibrium, which is called neutron star matter.

Once the solution has been found, the equation of state can be calculated from,

$$\begin{aligned} \epsilon = {} & \tfrac{1}{2}m_\sigma^2\sigma^2 + \tfrac{1}{2}m_\omega^2\omega_0^2 + \tfrac{1}{2}m_\rho^2\rho_{03}^2 \\ & + \sum_B \frac{2J_B + 1}{2\pi^2} \int_0^{k_B} \sqrt{k^2 + m_B^{\star\,2}}\, k^2\, dk \\ & + \sum_\lambda \frac{1}{\pi^2} \int_0^{k_\lambda} \sqrt{k^2 + m_\lambda^2}\, k^2\, dk, \end{aligned} \tag{17}$$

which is the energy density while the pressure is given by,

$$
\begin{aligned}
p &= -\tfrac{1}{2}m_\sigma^2\sigma^2 + \tfrac{1}{2}m_\omega^2\omega_0^2 + \tfrac{1}{2}m_\rho^2\rho_{03}^2 \\
&\quad + \frac{1}{3}\sum_B \frac{2J_B+1}{2\pi^2}\int_0^{k_B} k^4\,dk/\sqrt{k^2+m_B^{\star\,2}} \\
&\quad + \frac{1}{3}\sum_\lambda \frac{1}{\pi^2}\int_0^{k_\lambda} k^4\,dk/\sqrt{k^2+m_\lambda^2}.
\end{aligned} \tag{18}
$$

The theory is simper to solve in the case of symmetric nuclear matter, and this is a necessary first step in determining the coupling constants from the saturation properties. For nuclear matter near saturation, we simply fix $k_n = k_p = k$. The scalar and vector coupling constants can then be fixed by the known saturation density, ρ_0 and binding $B/A = (\epsilon/\rho)_0 - m_n$. The symmetry energy coefficient is,

$$
\begin{aligned}
a_{sym} &= \frac{1}{2}\left(\frac{\partial^2(\epsilon/\rho)}{\partial t^2}\right)_{t=0} \\
&= \left(\frac{g_\rho}{m_\rho}\right)^2 \frac{k_0^3}{12\pi^2} + \frac{k_0^2}{6(k_0^2+m^{\star 2})^{1/2}} \\
t &\equiv (\rho_n - \rho_p)/\rho
\end{aligned} \tag{19}
$$

and serves to fix the ρ-coupling. In the above equation, k_0 denotes the Fermi momentum of symmetric nuclear matter at saturation, ρ_0. The coupling constants that yield the following properties of symmetric nuclear matter,

$$
\begin{aligned}
\rho_0 = 0.16\ \mathrm{fm}^{-3},\quad B/A = -16.0\ \mathrm{MeV},\quad a_{sym} = 32.5\ \mathrm{MeV}, \\
\mathrm{K} = 265\ \mathrm{MeV},\quad m^\star_{sat}/m = 0.796
\end{aligned} \tag{20}
$$

are,

$$
(g_\sigma/m_\sigma)^2 = 8.63,\quad (g_\omega/m_\omega)^2 = 4.11,\quad (g_\rho/m_\rho)^2 = 4.54\ \ \mathrm{fm}^2. \tag{21}
$$

The first three properties determine the coupling constants, and the last two properties then follow automatically from the structure of the Lagrangian. It is remarkable that they are so close to the empirical values [14, 15], although the effective mass is perhaps slightly too large [16].

For use later in discussing the lambda hyperon binding in nuclear matter we note that the values of the scalar and vector field strengths at saturation are,

$$
S \equiv g_\sigma\,\sigma = 1.08\ \mathrm{fm}^{-1}, \qquad V \equiv g_\omega\,\omega_0 = 0.660\ \mathrm{fm}^{-1} \tag{22}
$$

The solution to the equations discussed above for neutron star matter, with hyperon to baryon coupling strength (discussed later), $x_\rho = x_\omega = x_\sigma \equiv g_{H\sigma}/g_{N\sigma} = \sqrt{2/3}$, is shown in Figs. 1,2, where the meson field amplitudes and chemical potentials are shown in the one, and the particle populations (in lieu of Fermi momenta) are shown in the other, both as functions of baryon density. It is interesting to compare

these with the fictional case that the only baryons are neutrons as in Fig. 3. In particular notice that the electron chemical potential increases monotonically as a function of density, whereas when the hyperons are taken into account it saturates at about 200 MeV. It is also interesting to see how the composition of dense charge-neutral matter is complex, as compared to the case where the hyperons are ignored. Even the neutron population is drastically altered, being little more populous than the proton or Λ at high density. The lepton populations are also drastically reduced by the hyperons because charge neutrality can be achieved among the baryons to high degree. This could have important effects on estimates of the transport properties of neutron star matter, in particular the conductivity and the viscosity. These are vital properties that effect the stability to rotation by damping gravitation radiation-reaction instabilities.

Table 1: Baryons and their charge states. Spin is J, isospin is I, its third component I_3, charge is q and strangeness is s.

	m (MeV)	J	I	I_3	q	s
N	939	1/2	1/2	-1/2	0	0
				1/2	1	0
Δ	1232	3/2	3/2	-3/2	-1	0
				-1/2	0	
				1/2	1	
				3/2	2	
Λ	1115	1/2	0	0	0	-1
Σ	1190	1/2	1	-1	-1	-1
				0	0	
				1	1	
Ξ	1315	1/2	1/2	-1/2	-1	-2
				1/2	0	
Ω	1673	3/2	0	0	-1	-3

In Fig. 4 we show the equation of state for three cases, pure neutron matter, beta equilibrium between neutrons, protons and leptons and equilibrium between all baryons to convergence with leptons. It is evident that pure neutron matter is not the lowest energy state of dense charge neutral matter and that the existence of hyperons considerably softens the equation of state, by relieving the Fermi pressure of the nucleons. In the last case, in actual fact, the baryon species populated to the highest densities in these neutron star models are the nucleons and hyperons of Table 1 with the exception of the Ω whose mass is so large that it lies above the chemical potential. The Δ is not populated for the same reasons given in ref. [11] which can be understood in terms of the isospin symmetry of the nuclear forces acting within the absolute constraint of charge neutrality. Briefly, the most favored charge state, the Δ^- is *isospin* unfavored by its large negative projection, $-3/2$ (same sign as the

neutron), while the isospin favored state,+3/2, the Δ^{++}, is doubly *charge* unfavored (same sign as proton). The threshold condition can be read from eq. (9),

$$\mu_n - q_B\mu_e \geq g_{\omega B}\omega_0 + g_{\rho B}\rho_{03}I_{3B} + m_B^\star \tag{23}$$

and the field amplitudes appearing in it can be found in Fig. 1.

3 Neutron Star Structure

The equations for the structure of a relativistic spherical and static star composed of a perfect fluid were derived from Einstein's equations by Oppenheimer and Volkoff [17]. They are,

$$4\pi r^2 dp(r) = -\frac{M(r)dM(r)}{r^2}\left(1+\frac{p(r)}{\epsilon(r)}\right)\left(1+\frac{4\pi r^3 p(r)}{M(r)}\right)\left(1-\frac{2M(r)}{r}\right)^{-1} \tag{24}$$

$$dM(r) = 4\pi r^2 \epsilon(r)\, dr. \tag{25}$$

(We use gravitational units, $G = c = 1$.) Given an equation of state, they can be integrated from the origin as an initial value problem for a set of arbitrary choices of the central density. Therefore they define a one parameter family of stars. The equation of state computed in this work needs to be supplemented by a sub-nuclear equation of state , and our choice in this work is the same as described in ref. [11]. Corresponding to the three equations of state of Fig. 4, we show the three families of neutron stars in Fig. 5. The equation of state for the case of pure neutron matter lies above the other two because a pure neutron state is not the lowest energy state of charge neutral matter. A state containing an equilibrium mixture of nucleons and leptons is lower and one containing an equilibrium population of all baryons to convergence is even lower. The latter two equations of state are coincident up to the threshold density of the first heavier baryon state beyond the nucleons. These features are also registered in the corresponding family of stars for the three cases.

The equations of star structure have to be integrated to the radius at which the pressure is zero, or very small compared to the central pressure. This means that the nuclear equation of state has to be supplemented by one corresponding to sub-nuclear densities. As described in ref. [11] we use that of Negele and Vautherin [18] for the sub-nuclear region of very neutron rich nuclei, and of Harrison and Wheeler [19] for the lower density crystaline lattice bathed in relativisitic electrons.

3.1 Baryon Populations

The populations of the maximum-mass star as a function of radius are shown in Fig. 6 for the case of full equilibrium of all baryons. Although the neutron is the dominant of the populations, the core contains a significant number of hyperons. Indeed the number of hyperons in the inner core exceeds by a small amount the total of the number of neutrons and protons. However integrated over the whole star the

hyperons amount to 29 % of the baryon population in this maximum mass model, the protons to 17%. Nevertheless the hyperons alter drastically the interior, up to a radius of 6-7 km, shifting negative charge from leptons to hyperons as can be seen by comparison with Fig. 7. This will certainly effect the electrical conductivity of the star which is relevant to the decay rate of the magnetic field of pulsars.

3.2 Hyperon Couplings: Constraints from Hyperon Binding in Nuclei

The ratio of hyperon to nucleon couplings to the meson fields,

$$x_\sigma = g_{H\sigma}/g_\sigma, \qquad x_\omega = g_{H\omega}/g_\omega, \qquad x_\rho = g_{H\rho}/g_\rho \tag{26}$$

are not defined by ground state properties of nuclear matter and so must be chosen according to other considerations. (For brevity we call $g_{N,\sigma}$ simply g_σ.) In studies of hypernuclear levels [20, 21, 22] these ratios are typically taken to be equal. In that case, small values between 0.33-0.4 are required. These are too small as regards neutron star masses, as is shown in Fig. 8. Recall that the most accurately determined mass (but not necessarily the maximum possible mass) is that of PSR1913+16 with $M/M_\odot = 1.442 \pm 0.003$ [23]. There is another relevant measurement, that of 4U0900-40 with $M/M_\odot = 1.85 \pm 0.3$ [24]. However the error is so large that many authors take the smaller mass as the limit. The actual number of known masses at the present time is less than 10 so that we cannot exclude that a more massive neutron star will be found. However to the imperfect extent to which the type II supernova mechanism is understood, there is support from the creation mechanism for a maximum possible mass of $\sim 1.5 M_\odot$.

The hyperons are actually more *strongly* populated in dense neutron star matter, the equation of state correspondingly softened, and the limiting mass reduced, the *weaker* their coupling to the meson fields [7, 9]. Indeed, even if the coupling is reduced to zero as for a Fermi gas model, but allowing the populations to reach equilibrium under the weak interactions, the hyperons are computed to be present in dense neutron star matter[25]. We can understand the increase of hyperon populations with a decrease in coupling in theories with long-range attraction and short-range repulsion as follows; above nuclear saturation density, the vector meson repulsion dominates the scalar meson attraction. If the hyperon coupling is weaker than the nucleon, the vector field amplitude can be reduced, by the shifting the baryon populations in favor of those with the weaker coupling, as is clear from eq. (5). This in turn lowers the energy by reducing the repulsive vector contribution, $\frac{1}{2}m_\omega^2\omega_0^2$, in eq. (17): weakening the coupling in dense matter amounts therefore to weakening the repulsion.

As noted above, when hypernuclear levels are analyzed with the constraint $x_\sigma = x_\omega$, the result is a small hyperon coupling leading to a neutron star family with much too small a limiting mass. However one is not compelled to take the ratios in eq. (26) to be equal, but there are large correlation errors in x_σ, x_ω in the published analysis of hypernuclear levels that take them unequal [22]. The analysis of hypernuclear levels could probably be improved by taking account of the rather well determined binding

energy of the Lambda hyperon in saturated nuclear matter. As noted elsewhere [26], this serves to strictly correlate the values of x_σ, x_ω but leaves a continuous pairwise ambiguity which hypernuclear levels may resolve. At the level of the published anaysis, which does not take account of the one to one relation between these parameters that is imposed by the Lambda binding, they do so only within a rather large range. In ref. [27] the binding of the Lambda hyperon in nuclear matter is inferred to be -28 MeV. We derive now the expression for this binding in our model. From the Weisskopf [28] relation at saturation between the Fermi energy and the energy per nucleon of a self-bound system, $e_F = (\epsilon/\rho)_0$, which is a special case of the Hugenholtz-Van Hove theorem [29], we obtain for the binding energy of the lowest Λ level in nuclear matter,

$$\begin{aligned}\left(\frac{B}{A}\right)_\Lambda &= x_\omega V + m_\Lambda^\star - m_\Lambda \\ &= x_\omega V - \frac{x_\sigma S}{1 + x_\sigma S/(2m_\Lambda)},\end{aligned} \tag{27}$$

where S, V were defined and their values given in eq. (22) and we have used eqs. (4,16). The first line holds for both the linear and non-linear $\sigma - \omega$ theories as well as this one. The second line specializes to this one. Thus as far as the lambda binding in nuclear matter is concerned, the scalar and vector ratios x_σ, x_ω need not be equal, but when so, they must be small, about 0.37. We show a few typical values in Table 2. According to the discussion above it is clear that for the larger values of x_ω in this table, the family of neutron stars will have a limiting mass star that exceeds the present observed lower bound of $M/M_\odot \sim 1.5$, as shown also in the table. However there are additional constraints that can be invoked. There is good reason to believe [30] that these ratios are less than unity. Moreover, according to the analysis of hypernuclear levels in finite nuclei, it is found that when the ratios are taken unequal the maximum likely value is $x_\sigma < 0.719$ [22]. It is not clear how strong this last constraint is, because it applies to the non-linear field theory [5] whose results would carry over only approximately to the present one. In any case, for such relatively simple theories of matter, perhaps one should not insist that when the interest is focused on bulk matter, the properties of finite nuclei are compelling constraints. The main point is that for a range of hyperon couplings that are compatible with the binding of the Lambda hyperon in nuclear matter, the corresponding families of neutron stars have limiting masses which exceed the presently observed lower bound on it. This is true also when the coupling is constrained by the analysis of hypernuclear levels, provided the analysis does not constrain x_σ to be equal to x_ω.

We have assumed that other hyperons in the lowest octet have the same coupling as the Lambda, and also we have arbitrarily taken $x_\rho = x_\sigma$. This choice produces results very close to another possible one, $x_\rho = x_\omega$.

As a final point on this subject, the limiting neutron star mass (and those below it) are much more sensitive to the value of x_ω than x_σ. For example the limiting mass for the entry of the table, $x_\sigma = 0.8, x_\omega = 1.0$, differs from the choice $x_\sigma = x_\omega = 1$ by only 5 percent. Thus for example, any choice of $x_\omega > 0.8$ is compatible with neutron star masses and the Lambda binding in nuclear matter.

Table 2: Values of the hyperon to nucleon scalar and vector coupling that are compatible with the binding of -28 MeV for lambda hyperons in nuclear matter and the corresponding maximum neutron star mass.

x_σ	x_ω	$M/M_\odot$
.3	.262	1.08
.4	.415	1.13
.5	.566	1.23
.6	.714	1.36
.7	.859	1.51
.8	1.00	1.66
.9	1.14	1.79
1.	1.27	1.88

3.3 Mass-Radius Relation, Kepler Frequency, Moment of Inertia

The mass-radius relation is an important one because it can be used to estimate how rapidly the stars in the family belonging to a given equation of state can rotate without shedding mass at the equator. Such relations for the three cases of Fig. 8 are shown in Fig. 9. The curves marked in milliseconds are such that stars falling below a given curve can rotate without mass loss to at least the period marked on the curve. These periods correspond to the relativistic Kepler frequency *of the limiting mass star* in the sequence belonging to an equation of state, and can be approximated [31, 32] by

$$\Omega_K \approx 0.65\Omega_c, \qquad \Omega_c = \sqrt{\frac{M}{R^3}} = 3.7 \times 10^5 \sqrt{\frac{M/M_\odot}{(R/\mathrm{km})^3}}\ \mathrm{s}^{-1}, \tag{28}$$

where Ω_c is the Newtonian Kepler frequency at which centrifuge and gravity balance. The factor, 0.65, is empirical, approximate, and is particular to typical limiting-mass neutron star models, and has its origin in the general relativistic dragging of the local inertial frame [33], the centrifulgal effects being determined by the difference in the angular velocity of the star and the angular velocity of the local inertial frames [34]. We see from the figure that some stars in all these families can rotate at 1.5 ms but none at 0.5 ms so far as the limitation of mass loss at the equator is concerned.

We have also carried out a general relativistic calculation of the Kepler frequency using the Hartle-Thorne perturbative method of solving the equations for rotating stellar structure [35, 34]. When this method is supplemented by a self-consistency condition on the frequency that was first introduced into the method in ref. [36], the perturbative method is found to be in accord with an exact numerical calculation of Einstein's equations, as shown in ref. [33], up to the highest frequency that neutron stars, limited by gravity wave instabilities, can have [37].

The ingredient missing from earlier applications of Hartle's method is the transcendental equation for the general relativistic Kepler frequency. It is given by [38]

$$\Omega_K = e^{\nu-\psi}\ V(\Omega_K) + \omega(\Omega_K)\,, \tag{29}$$

$$V(\Omega_K) \equiv \frac{\omega'}{2\psi'}\,e^{\psi-\nu} + \sqrt{\frac{\nu'}{\psi'} + \Big(\frac{\omega'}{2\psi'}\,e^{\psi-\nu}\Big)^2}\,. \tag{30}$$

Equations (29) and (30) are to be evaluated at the star's equator. The quantity V denotes the orbital velocity measured by an observer with zero angular momentum in the ϕ-direction. Primes refer to derivatives with respect to the radial coordinate. The quantity ω denotes the frequency of the local inertial frame (dragging effect). An essential feature is that V and ω (like the metric functions ν and ψ) depend on Ω_K. Therefore to find the Kepler frequency, a self-consistent solution of Hartle's equations that satisfies the above transcendental relation for Ω_K must be constructed. Details of how this can be done are given in ref. [36].

We show the relativistic Kepler frequency for the sequence of stars belonging to $x = \sqrt{2/3}$ in Fig. 10 and compare it with the classical result, Ω_c of eq. (28). The relativistic frequency is lower than the classical one because of the phenomenon in general relativity known as dragging of the local inertial frame by the rotation of the star. While unimportant in most stars, it becomes significant in rapidly rotating neutron stars. The centrifugal effects are given by the excess of the rotational frequency of the star over the (radially dependent) frame dragging frequency. Also shown in the figure is the case discussed in the next section in which the core of the star is in the mixed phase of hadronic and quark matter. This figure also shows how the limiting mass of a sequence belonging to a particular equation of state is increased by rotation at the Kepler frequency, from $1.5M_\odot$ to $1.7M_\odot$, in the case of the star at the limit.

It is relevant to note that the shortest period so far observed is 1.6 ms for PSR1937+21, discovered in 1982 [39]. It is clear that this period poses no constraint on the theory of matter when the shortest period is estimated as the Kepler (mass shedding) period. We will later discuss gravitational radiation instabilities that limit the shortness of the period of rotation even more severely than mass shedding.

The moment of inertia in general relativity is given by,

$$I = \frac{8\pi}{3}\int_0^R dr\ r^4\ \frac{(\epsilon(r)+p(r))}{\sqrt{1-2m(r)/r}}e^{-\Phi(r)}\frac{\Omega-\omega(r)}{\Omega}, \tag{31}$$

where $\omega(r)$ is the angular velocity of the local inertial frame (frame dragging), and for slow rotation is much smaller than the stars angular velocity, Ω. We therefore neglect it in the calculation of I. The function $\Phi(r)$ is related to the metric function $g_{00} = e^{2\Phi}$ and is the solution of,

$$\frac{d\Phi}{dr} = \frac{m(r)+4\pi r^3 p(r)}{r(r-2m(r))}, \tag{32}$$

with boundary condition,

$$2\Phi(R) = \ln\Big(1-\frac{2M}{R}\Big), \tag{33}$$

where M, R are the star's mass and radius. For the three couplings of hyperons of Fig. 8 we show the moment of inertia in Fig. 11. Little is known about the moments of inertia of neutron stars. However, assuming as is likely, that the energy required to power the crab nebula, about 4×10^{38} erg s^{-1}, is provided by the loss of rotational energy by the pulsar, its moment of inertia is at least $40 M_\odot$ km^2 [40]. This can be accounted for by all of the couplings shown in this figure.

There is a constraint relating the mass and surface redshift as determined from gamma-ray bursters. It is at present a very weak constraint because the redshift is not measured for any neutron star whose mass is also known. All we know is that the surface redshifts seem to lie in the range $z \equiv \Delta\lambda/\lambda = 0.2 - 0.5$ [41] while masses seem to lie in the range $M/M_\odot = 1 - 1.85$ with an error of ± 0.3 at both ends [24]. In any case, eventually a redshift for a star whose mass is also known may be measured, so we show in Fig. 12 the surface redshift

$$z = 1/\sqrt{1 - 2M/R} - 1, \tag{34}$$

as a function of mass.

4 Hybrid Quark-Neutron Star

Many authors have discussed the possibility that the dense interior of neutron stars may be converted to quark matter [42, 43]. If so, it must be strange quark matter, since 3-flavor quark matter has lower energy than 2-flavor and just as in the discussion of the hyperon content of neutron stars, strangeness is not conserved on macroscopic time scales. Such stars we call hybrids. Many of the earlier discussions [42] have treated the neutron star as pure in neutron, and the quark phase as consisting of the equivalent number of u and d quarks. As seen above, pure neutron matter is not the ground state of the star, nor is a mixture of $n_d = 2n_u$ the ground state of quark matter. In fact it is a highly excited state, and will quickly weak decay to an approximately equal mixture of u,d,s quarks. Several others have included the presence of many baryons in equilibrium in the confined phase but have approximated the mixed phase as two components which are separately charge neutral [43]. Both of these approximations have hidden an interesting aspect of the discussion of hybrid stars, which we briefly outline here and which is treated fully elsewhere[44]. First we discuss the case of a star made from purely neutron matter so as to contrast it with one made from beta stable neutral matter. Since charge neutrality is automatically satisfied by pure neutron matter, it is characterized by a single chemical potential, that for the neutrons. The Gibbs phase equilibrium point can then be expressed as the solution for μ of,

$$p_H(\{\phi\}, \mu, T) = p_Q(\mu, T), \tag{35}$$

where the subscript H, Q denotes hadronic confined and quark phases respectively and $\{\phi\}$ denotes the field variables and Fermi momenta that characterize a solution to the equations of confined hadronic matter exclusive of the chemical potential.

(Analogous variables in principle would characterize the other phase. However we shall use the bag model to describe the quark phase. In this case the state of this phase is characterized by the chemical potential(s) and temperature.) The baryon densities, ρ_H, ρ_Q, and the energy densities, ϵ_H, ϵ_Q, in the two phases at the solution, μ, of the above equation (phase equilibrium) are different since they are different functions of μ, and the proportion of the two components varies between ρ_H and ρ_Q. The pressure and chemical potential are equal in the two phases in equilibrium and remain *constant* between these two densities, as expressed in the above equation, which is a characteristic feature of phase equilibrium in a system for which there is a single chemical potential. This is the usual text book example of phase equilibrium [45]. In the absence of gravity, the two phases will occupy separate but intermixed regions. The size and shape of the regions (spheres, rods, slabs..) is determined by the surface and Coulomb energies and the geometry will vary as the concentrations. The constancy of the pressure in the mixed phase in this simple first order phase transition would have a particular consequence in a star if it were an appropriate description of the transition. The mixed phase could not exist in a star since the star's pressure is a monotonic decreasing function from the inside out, eq. (24). That is to say, the mixed phase at one density cannot support against gravity, the mixed phase at a higher density when the pressure is the same at both densities. The denser component sinks (just as in a pot of hot water in equilibrium with the vapor, under the influence of the earth's gravitational field). The mixed phase would be squeezed out by gravity! Consequently the density profile of the star would suffer a discontinuity, falling from ρ_Q to ρ_H at the radius in the star where the pressure attains the value of the phase equilibrium pressure, just as in the analogy with the pot of water in the earth's gravitational field. However this is purely an artifact of the treatment of the phase transition as if it were characterized by a single chemical potential (for baryon number).

We now contrast this with the case of the phase transition between confined hadronic matter and quark matter both in beta equilibrium and with the *two* conservation laws for baryon and electric charges properly taken into account. The confined hadronic matter is described above, and the deconfined quark matter phase by the bag model described below.

When the body that undergoes a first order phase transition has two or more conserved charges (additive attributes of the constituents) then, as developed previously [44] phase equilibrium is no longer a point in the pressure chemical-potential plane. This is because the Gibbs condition written earlier with one chemical potential, eq. (35), does not by itself provide a unique solution when there are two (or more) chemical potentials in it. The Gibbs equation appropriate to a first order phase transition in a neutron star in beta equilibrium (or any other body containing more than two conserved charges) is

$$p_H(\{\phi\}, \mu_n, \mu_e, T) = p_Q(\mu_n, \mu_e, T). \tag{36}$$

This equation describes a curve, not a point in the three dimensional space of p, μ_n, μ_e when supplemented by the conservation condition on charge. When the phases are in equilibrium the body consists partly of one phase and partly the other. Let χ lying

in the range (0,1) parameterize the proportion of total volume occupied by the quark phase. Charge neutrality in this mixed phase is enforced by

$$(1-\chi)q_H(\{\phi\},\mu_n,\mu_e,T)+\chi q_Q(\mu_n,\mu_e,T)+q_e(\mu_e,T)=0, \tag{37}$$

which can be thought of as defining μ_e as a particular function, $\mu_e = f(\mu_n,\chi,\{\phi\},T)$ of μ_n. When μ_e is determined by this equation then the curve that eqs. (36) describes is the phase equilibrium curve along which the density (controlled by μ_n) and pressure (a function of μ_n and μ_e) vary while the charge remains zero. Note however that eq. (37) couples the hadronic and quark phases for χ lying between the extremes of its range, so that the equations of motion of *both* phases must be solved *simultaneously* with eq. (36) and (37) in the mixed phase. Therefore the solution, meaning the field variables, chemical potentials, pressure and densities, vary as the concentration! This is unlike phase transitions with only one conserved quantity (eg. H_2O in the gas-liquid transition), where the pressure, chemical potentials, and densities of both phases in equilibrium remain constant until the entire body converts from one phase to the other. The energy density and baryon density in the mixed phase are the same linear combinations of the two phases as the charge,

$$\epsilon=(1-\chi)\epsilon_H(\{\phi\},\mu_n,\mu_e,T)+\chi\epsilon_Q(\mu_n,\mu_e,T) \tag{38}$$

$$\rho=(1-\chi)\rho_H(\{\phi\},\mu_n,\mu_e,T)+\chi\rho_Q(\mu_n,\mu_e,T). \tag{39}$$

but because of eq. (37), μ_e depends on χ so that the energy and density are not linear functions of the concentration as in a simple substance. Phase equilibrium requires that only the pressure, chemical potentials and temperature are the same in the two phases in contact. Therefore the characteristic discontinuity in density across the interface of the two phases in equilibrium exists

$$\Delta(\chi)=\rho_H(\{\phi\},\mu_n,\mu_e,T)-\rho_Q(\mu_n,\mu_e,T), \tag{40}$$

but, in the general case, it too varies as the concentration, whereas in a simple substance it remains a constant. In complex substances, ones with more than one conserved charge, the discontinuity tends to be small because the density of each phase in equilibrium varies as the concentration so that the discontinuity does not amount to the difference in densities at the extremes of the mixed phase, as in the case of a simple substance [44]. For this reason, although the mixed phase will undoubtedly develop geometrical structure, just as is expected of the sub-nuclear liquid-vapor transition [46, 47], the energy associated with it is likely to be small in comparison with the volume energy [44]. Therefore we do not enter into a discussion of it here, since it cannot much effect the global properties on which we concentrate. Parenthetically we remark that the geometrical structure of the mixed phase may be very important for transport phenonena.

It remains to define what we take to be the description of quark matter. We follow Farhi and Jaffe [48] who find for the thermodynamic potential of massive quarks to $O(\alpha_c)$, renormalized at the scale ρ to be,

$$\Omega_f = -\frac{\gamma_f}{24\pi^2}\Big\{\mu_f\sqrt{\mu_f^2-m_f^2}(\mu_f^2-\frac{5}{2}m_f^2)+\frac{3}{2}m_f^4\ln\Big[\frac{\mu_f+\sqrt{\mu_f^2-m_f^2}}{m_f}\Big]$$

$$- \frac{2\alpha_c}{\pi}\Big[3\Big(\mu_f\sqrt{\mu_f^2-m_f^2}-m_f^2\ln\Big[\frac{\mu_f+\sqrt{\mu_f^2-m_f^2}}{\mu_f}\Big]\Big)^2-2\Big(\mu_f^2-m_f^2\Big)^2$$

$$-3m_f^4\ln^2\frac{m_f}{\mu_f} + 6\ln\Big(\frac{\rho}{\mu_f}\Big)\Big(\mu_f\sqrt{\mu_f^2-m_f^2}m_f^2-m_f^4\ln\Big[\frac{\mu_f+\sqrt{\mu_f^2-m_f^2}}{m_f}\Big]\Big)\Big]\Big\}, \quad (41)$$

where μ_f, m_f denote the chemical potential and mass of the quark flavor f, ($f = u, d, s, c$) and $\gamma_f = 2\times 3_{\text{color}}$ is the degeneracy. (A sign has been corrected in the above expression for Ω_f.) The renormalization scale, ρ should be typical of the chemical potentials of the problem and we set $\rho = 300$ MeV. We also take the u,d quark masses to be zero and the s quark mass to be 150 MeV. (Even in the most massive compact stars, the chemical potential does not approach the charmed quark mass at 1500 MeV.) The thermodynamic potentials for the electron (0.511 MeV) and muon (106 MeV) are given also by the above expression with the omission of the α_c terms, and the replacement of the degeneracy factor, γ_f by that of the leptons $\gamma_\lambda = 2$. The quark number densities, baryon number density, charge density, energy density and pressure are given by,

$$n_i = -\partial\Omega_i/\partial\mu_i \quad (42)$$

$$\rho = \frac{1}{3}\sum_{u,d,s,c} n_i \quad (43)$$

$$q_Q = \sum_i n_i q_i \quad (44)$$

$$\epsilon = B + \sum_i(\Omega_i + \mu_i n_i) \quad (45)$$

$$p = -B - \sum_i \Omega_i \quad (46)$$

where the sums, i, extend of all three quarks and the two leptons. The difference in the vacuum energy of confined and deconfined phases is denoted by B and q_i denotes the electric charge on the particle type $i = u, d, s, c, e^-, \mu^-$. Because of the long time-scale, strangeness is not conserved in the star so that the quark chemical potentials can be expressed in terms of the two conserved charges, baryonic and electric,

$$\mu_u = \frac{1}{3}(\mu_n - 2\mu_e), \qquad \mu_d = \mu_s = \frac{1}{3}(\mu_n + \mu_e), \quad (47)$$

Therefore at specified baryon number density and total charge density

$$q_Q(\mu_n, \mu_e) + q_e(\mu_n, \mu_e) \equiv 0, \quad (48)$$

of the pure quark matter phase the two independent chemical potentials, μ_n, μ_e can be determined and then the equation of state.

The mixed phase involves, as discussed above, the simultaneous solution of the coupled system. For the confined hadronic phase we must solve eqs. (5-12) except that eqs. (8) and (12) are replaced by eqs. (36) and (37). The solution defines the field variables, Fermi momenta of the baryons and leptons and the two independent

chemical potentials, the latter being sufficient in this model of quark matter to specify its state. This has to be done for a number of different concentrations χ.

We do not carry out an exhaustive exploration of the parameters of the bag model but fix $B^{1/4} = 180$ MeV and $\alpha_c = 0.2$ since this choice places the equilibrium energy per baryon of strange quark matter at $E/A = 1100$ MeV, well above the energy per nucleon in Fe^{56}. (Two-flavor quark matter is at $E/A = 1200$ MeV.) The lower density end of the mixed phase of confined hadronic matter and deconfined strange quark matter is at 0.334 fm^{-3}, about twice normal nuclear density. The mixed phase ends and the pure strange quark phase begins at 1.54 fm^{-3}, a much higher value than obtains in the approximation that the confined phase consists of pure neutron matter (where there is a single conservation law, that for baryon number) [44]. The above results for the phase transition refer to the choice of universal coupling in the confined hadronic phase. (According to the discussion is subsection 3.2 the star properties are dominated insofar as the couplings are concerned by the $\omega-$meson and so this choice is consistent with the Lambda binding of the sixth entry in Table 2.)

In contrast to the familiar phase transition like a liquid-gas transition, in which the pressure remains a constant for all concentrations of the two phases in equilibrium, we see here a different behavior. When there are two (or more) conserved quantities in a system that undergoes a phase transition, such as the confined-deconfined phase transition in a star, then the mixed phase occurs for a *range* of values of the neutron chemical potential, and the pressure and electron chemical potential vary continuously through the mixed phase, both as a function of μ_n and as a function of baryon density. Fig. 13 shows the variation of these quantities. The pure confined and deconfined phases lie at densities below and above the vertical lines, respectively, and the mixed phase of these two components lies between. The family of hybrid stars is shown in Fig. 14. Those below the point marked 'm' are pure neutron stars, and those above have cores that are in the mixed phase with mantles that are in the confined phase. The pure quark phase occurs in the inner cores of stars that lie above the point marked 'm'', but these stars have central densities beyond the maximum mass star and so are unstable [19]. The baryon mass, the mass of the equivalent number of neutrons dispersed to infinity, lies above the gravitational mass for the entire family. The difference is the binding energy of the star. The hadronic and quark composition of the star at the mass limit is shown in Fig. 15. The entire core of the star out to 7.6 km is in the mixed phase. The central density does not approach that required for a complete conversion to quark matter. The outer mantle of the star from 7.6 km to 10.2 km is in the pure confined phase. Of the total baryon number of the maximum mass hybrid star, 57 % are neutrons, 16 % protons, 5 % hyperons and 22 % quarks. The net charge on the baryons is positive, as would be expected due to the isospin symetric nuclear force, and on the quarks it is negative. The very small lepton number completes the charge neutrality of the star.

The lepton populations in the hybrid star of Fig. 15 are even more severely reduced compared to a star for which the phase transition has not occured, as in Fig. 6. The transport properties estimated for neutron stars treated as containing only neutrons, protons and electrons, as in Fig. 7, must be quite different than those properties in stars in which full beta equilibrium is taken into account, and in which perhaps, as in

this example, the mixed two-component phase of confined and quark matter occupies the core of the star.

If strange quark matter is the absolute ground state, then of course the structure of compact stars is quite different in the case that the central density lies above the lower threshold of the mixed phase. Such stars would convert entirely to strange stars. (See ref. [49] for more discussion and references.)

5 Gravitational Radiation-Reaction Instability

The Kepler frequency, above which centrifuge overwhelms gravity at the equator of a rotating star, provides only an absolute upper bound on frequency. There is another instability that sets in at lower frequency which therefore provides a more stringent and realistic limit [50]. It originates in counter-rotating surface vibrational modes, which at sufficiently high rotational frequency of the star are dragged forward. In this case, gravitational radiation which inevitably must accompany the aspherical transport of matter, does not damp the modes, but rather drives them [51, 52]. Viscosity plays the important role of damping such gravitational-wave driven instabilities at a sufficiently reduced frequency such that the viscous damping rate and power in gravity waves are comparable [53]. We have found recently that these viscosity modified GR instabilities may set in at a significantly small fraction (60-70%) of the Kepler frequency and therefore set a more realistic upper bound than the latter [36, 37].

Of course the normal modes of a star corresponding to a specific equation of state are numerically very difficult to obtain, and approximation schemes based on Maclaurin spheroids have been developed. The modes are taken to have the dependence $\exp[i\omega_m(\Omega)t + im\phi - t/\tau_m(\Omega)]$ where ω_m is the frequency of the $m = l$ surface mode which depends also on the angular velocity, Ω of the star, ϕ is the azimuthal angle and τ_m is the time scale for the mode which determines its growth or damping. The rotation frequency Ω at which it changes sign is the critical frequency for the particular mode, m. It is conveniently expressed as the frequency, Ω_m, that solves [50],

$$\Omega_m = \frac{\omega_m(0)}{m}\left[\alpha_m(\Omega_m) + \gamma_m(\Omega_m)\left(\frac{\tau_{G,m}}{\tau_{V,m}}\right)^{1/(2m+1)}\right]. \tag{49}$$

In this equation, the frequency of the vibrational mode in a non-rotating star is given by [54]

$$\omega_m(0) = \Omega_c\sqrt{\frac{2m(m-1)}{2m+1}}; \tag{50}$$

where Ω_c was given in eq. (28). The time scale for gravitational radiation reaction is [55]

$$\tau_{G,m} = \frac{2}{3}\frac{(m-1)[(2m+1)!!]^2}{(m+1)(m+2)}\left(\frac{2m+1}{2m(m-1)}\right)^m \Omega_c^{-2(m+1)}R^{-(2m+1)}, \tag{51}$$

and that for viscous damping is [56]

$$\tau_{V,m} = \frac{R^2}{(2m+1)(m-1)} \frac{\overline{\rho}}{\eta}, \tag{52}$$

where $\overline{\rho} = M/(\frac{4}{3}\pi R^3)$. The shear viscosity is denoted by η and depends on the temperature of the star, being small in very hot and therefore young stars and larger in cold stars. The functions α_m and γ_m contain information about the pulsation of the rotating star models and are difficult to determine [50, 57]. However it turns out that they are rather weakly dependent on the equation of state, and are close to unity and have sometimes been approximated as such. Here we take $\alpha_m(\Omega_m)$ and $\gamma_m(\Omega_m)$ as calculated in ref. [58, 59] (for the oscillations of rapidly rotating inhomogeneous Newtonian stellar models; polytropic index n=1) and ref. [50] (for uniform-density Maclaurin spheroids, i.e. n=0), respectively. In the above approximation scheme, the properties of the particular model star enter through its mass and radius which occur in the above equations, not on other details of the equation of state except insofar as it determines these quantities. Indeed, in a study of polytropes, it has been confirmed that Ω_m depends much more strongly on the radius and mass of the neutron star model (through $\Omega_c, \tau_{V,m}$ and $\tau_{G,m}$) than on the polytropic index assumed in calculating α_m [60].

To relate the temperature and viscosity of a star we adopt the expression [61, 57],

$$\eta = 347\overline{\rho}^{9/4}/T^2, \tag{53}$$

where $\overline{\rho}$ is the density in g/cm^3, T is temperature in Kelvin and η is the shear viscosity in g/(cm s). Bulk viscosity has a different temperature dependence [62] and may be important at high temperature before it falls below $T \sim 10^{11}$ K in a newly born star. If so, then the minimum stable period of a hot star could be less than our estimate.

In Fig. 16 is shown the minimum stable period that the family of neutron stars corresponding to hyperon coupling $x = \sqrt{2/3}$ can have in the face of viscosity moderated gravitation-reaction instabilities. It is a very strong function of the mass and radius of the star. The minimum stable period of a hot star establishes the limit of the star during its life time so long as it is isolated and remains so. (The presence of a binary companion is easily detected in the frequency modulation of the pulses of a pulsar.) For the limiting mass star the minimum period is about 1 ms. It is a strong function of the mass of the star, through the dependence on radius. For comparison, from Fig. 10, the Kepler period of the limiting mass star is $P \sim 0.63$ ms (and similarly for the hybrid star). So the gravity wave instabilities set a much more stringent limit on stable rotation than the mass shedding limit for stars whose history has left them isolated from a companion. The $T = 10^6$ K curve of Fig. 16 is relevant to old cold stars that have acquired a companion, and spin up by accretion. In this case the GR instability is closer to the Kepler mass-shedding instability. The corresponding results for the hybrid star family are nearly identical for the same range of viscosity used so we do not show them. Of course the relationship to the temperature through eq. (53) is not necessarily valid. The conclusion is the same: the minimum stable rotational period is about 1 ms and is a strong function of the mass of the star.

6 Summary

We have computed a number of neutron star properties corresponding to the derivative coupling Lagrangian involving the exchange of scalar, vector and vector-isovector mesons, which describes quite accurately the five bulk properties of symmetric nuclear matter in the mean field approximation. For the description of charge-neutral equilibrium matter (neutron star matter) we include all baryon states to convergence at the highest densities appearing in the corresponding neutron star models. These turn out to be nucleons and hyperons, but not deltas. Several different hyperon couplings were employed. The dependence is similar to that found in [11, 7, 9], namely, the smaller the hyperon to nucleon coupling, the more strongly the hyperons contribute. This seemingly inverted behavior actually is a logical consequence of the fact that the high density equation of state is dominated by the repulsion of the vector mesons. Hyperon couplings compatible with bounds placed by observed neutron star masses and by the binding of the Lambda hyperon in saturated nuclear matter are found. It is clear that the mass limit computed for neutron stars is sensitive to the presence of hyperons with coupling so chosen to agree with the empirical binding of the Lambda, and it is substantially below the value that would be obtained with their neglect.

The possible conversion of the core of the more massive members of the family of neutron stars to quark matter was considered. We emphasized the fact that for a star in beta equilibrium, two conservation laws (for electric charge and baryon number) should be enforced in determining the transition from confined to deconfined phases. This has the consequence that the pressure varies continuously for all admixtures of the two components throughout the mixed phase, and is *not* constant as in the well known liquid-gas transition, where there is only one conserved quantity, the number of H_2O molecules. Therefore if the phase transition conditions are achieved in a star, because of the pressure gradient in the mixed phase, the two components are not separated by gravity. In our example, even in the star at the mass limit, total conversion to the quark phase does not take place. However the mixed phase extends throughout most of the star.

We also computed the minimum rotational period imposed by gravitational radiation reaction instabilities, which is appreciably larger than the Kepler period, and therefore sets the minimum rotational period of neutron star models. According to our finding here and earlier [36, 37] the gravitational wave instability effectively limits the period of neutron stars to $P > 1$ ms unless, as cold stars, they have been spun up by accretion. Then the period can be slightly smaller. The period of the fastest pulsar known so far [39] with $P = 1.56$ ms is easily accommodated by the theory of dense matter discussed here whether or not a phase transition to quark matter has occurred.

Acknowledgements: This work was supported by the Director, Office of Energy Research, Office of High Energy and Nuclear Physics, Division of Nuclear Physics, of the U.S. Department of Energy under Contract DE-AC03-76SF00098. One of us (F.W.) acknowledges a fellowship from the Max Kade Foundation.

References

[1] M. Rho and D. Wilkinson, *Mesons in Nuclei*, vols. I, II and III, North Holland Publ. Co., Amsterdam, (1979).

[2] B. D. Serot and J. D. Walecka, *The Relativistic Nuclear Many-Body Problem*, in "Advances in Nuclear Physics", eds. J. W. Negele and E. Vogt, (Plenum Press N. Y.), 1986.

[3] L. S. Celenza and C. M. Shakin, *Relativistic Nuclear Physics*, World Scientific, Singapore, (1986).

[4] M. H. Johnson and E. Teller, Phys. Rev. **98** (1955) 783 ;
H. P. Duerr, Phys. Rev. **103** (1956) 469;
J. D. Walecka, Ann. of Phys. **83** (1974) 491.

[5] J. Boguta and A. R. Bodmer, Nucl. Phys. **A292** (1977) 413.

[6] J. Zimanyi and S. A. Moszkowski, Phys. Rev. C **42** (1990)1416.

[7] N. K. Glendenning, Nucl. Phys. **A493** (1989) 521.

[8] J. I. Kapusta, and K. A. Olive, Phys. Rev. Lett. **64** (1990) 13.

[9] J. Ellis, J. I. Kapusta and K. A. Olive, Nucl. Phys. **B348** (1991) 345.

[10] S. I. A. Garpman, N. K. Glendenning and Y. J. Karant, Nuc. Phys. **A322** (1979) 382.

[11] N. K. Glendenning, Astrophys. J. **293** (1985) 470.

[12] N. K. Glendenning, B. Banerjee and M. Gyulassy, Ann. Phys. (N. Y.) **149** (1983) 1.

[13] J. D. Bjorken and S. D. Drell, *Relativistic Fields*, McGraw Hill, N. Y., 1965.

[14] N. K. Glendenning, Phys. Rev. C **37** (1988) 2733.

[15] M. M. Sharma, W. T. A. Borghols, S. Brandenburg, S. Crona, A. van der Woude and M. N. Harakeh, Phys. Rev. C **38** (1988) 2562.

[16] M. Jaminon and C. Mahaux, Phys. Rev. C **40** (1989) 354.

[17] J. R. Oppenheimer and G. M. Volkoff, Phys. Rev. **55** (1939) 374.

[18] J. W. Negele and D. Vautherin, Nucl. Phys. **A178** (1973) 123.

[19] B. K. Harrison, K. S. Thorne, M. Wakano and J. A. Wheeler, *Gravitation theory and gravitational collapse*, (Chicago: University of Chicago Press) 1965.

[20] J. Boguta and S. Bohrmann, Phys. Lett. **102B** (1981) 93.

[21] G. E. Walker, Nucl. Phys. **A450** (1986) 287c.

[22] M. Rufa, J. Schaffner, J. Marhun, H. Stocker, W. Greiner and P.-G. Reinhard, Phys. Rev. C **42** (1990) 2469.

[23] J. H. Taylor and J. M. Weisberg, Astrophys. J. **345** (1989) 434.

[24] P. C. Joss and S. A. Rappaport, Ann. Rev. of Astr. and Astrophys. **22** (1984) 537.

[25] V. A. Ambartsumyan and G. S. Saakyan, Astron. Zh. **37** (1963) 193 [Soviet Ast. – AJ,**4** (1960) 187].

[26] N. K. Glendenning and S. A. Moszkowski, *Reconciliation of Neutron Star Masses and the Binding of the Lambda in Hypernuclei*, LBL-30645, April, 1991.

[27] D. J. Millener, C. B. Dover and A. Gal, Phys. Rev. C **38** (1998) 2700.

[28] V. F. Weisskopf, Rev. Mod. Phys. **29** (1957) 174.

[29] N. M. Hugenholtz and L. Van Hove, Physica **24** (1958) 363.

[30] S. A. Moszkowski, Phys. Rev. D **9** (1974) 1613.

[31] J. L. Friedman, J. R. Ipser and L. Parker, Phys. Rev. Lett. **62** (1989) 3015.

[32] P. Haensel and J. L. Zdunik, Nature **340** (1989) 617.

[33] F. Weber and N. K. Glendenning, *Applicability of Hartle's Method for the Construction of General Relativistic Rotating Neutron Star Models*, (LBL 29671, 1991).

[34] J. B. Hartle and K. S. Thorne, Astrophys. J. **153** (1968) 807.

[35] J. B. Hartle, Astrophys. J. **150** (1967) 1005.

[36] F. Weber, N. K. Glendenning and M. K. Weigel, (LBL-28845, May 1990) to appear in Astrophys. J., June 1991.

[37] F. Weber and N. K. Glendenning, (LBL-29141, June 1990) to appear in Z. Phys. A.

[38] J. L. Friedman, J. R. Ipser and L. Parker, Astrophys. J. **304** (1986) 115.

[39] D. C. Backer, S. Kulkarni, C. Heiles, M. M. Davis, W. M. Goss, Nature **300** (1982) 615.

[40] R. N. Manchester and J. H. Taylor, *Pulsars*, W. H. Freeman and Co., San Francisco, 1977.

[41] E. P. Liang, Astrophys. J. **304** (1986) 682.

[42] G. Baym and S. A. Chin, Phys. Lett. **62B** (1976) 241;
B. D. Keister and L. S. Kisslinger, Phys. Lett. **64B** (1976) 117;
G. Chapline and M. Nauenberg, Phys. Rev. D **16**(1977) 450;
W. B. Fechner and P. C. Joss, Nature **274** (1978) 347;
H. A. Bethe, G. E. Brown and J. Cooperstein, Nucl. Phys. **A462** (1987) 791;
B. D. Serot and H. Uechi, Ann. Phys. (N. Y.) **179** (1987) 272.

[43] N. K. Glendenning, in Int. Nucl. Phys. Conf., August 1989, Sao Paulo, Brasil, Vol. 2, p. 711, ed. by M. S. Hussein et al., World Scientific, Singapore, 1990;
N. K. Glendenning, in International Workshop on Relativistic Aspects of Nuclear Physics, August 1989, p. 241, ed. by T. Kodama et al., World Scientific Publishing Co., Singapore, 1990;
J. Ellis, J. Kapusta and K. A. Olive, Nucl. Phys. **B348** (1991) 345.

[44] N. K. Glendenning, *Phase Transitions with More than One Conserved Charge: Consequences for Neutron Stars.* LBL-30295 (1991).

[45] L. D. Landau and E. M. Lifshitz, *Statistical Physics*, ch. VIII, Addison-Wesley (1969).

[46] D. G. Ravenhall, C. J. Pethick and J. R. Wilson, Phys. Rev. Lett. **50** (1983) 2066;
D. G. Ravenhall, C. J. Pethick and J. M. Lattimer, Nucl. Phys. **A407** (1983) 571, and refernces cited.

[47] R. D. Williams and S. E. Koonin, Nucl. Phys. **A435** (1985) 844.

[48] E. Farhi and R. L. Jaffe, Phys. Rev. D **30** (1984) 2379.

[49] N. K. Glendenning, Mod. Phys. Lett. A, **5** (1990) 2197.

[50] L. Lindblom, Astrophys. J. **303** (1986) 303.

[51] S. Chandrasekhar, Phys. Rev. Lett. **24** (1970) 611.

[52] J. L. Friedman, Phys. Rev. Lett. **51** (1983) 11.

[53] L. Lindblom and S. L. Detweiler, Astrophys. J. **211** (1977) 565.

[54] W. Thomson, Phil. Trans. Roy. Soc. London, **153** (1863) 608.

[55] S. L. Detweiler, Astrophys. J. **197** (1975) 203.

[56] H. Lamb, Proc. London Math. Soc. **13** (1881) 51.

[57] C. Cutler and L. Lindblom, Astrophys. J. **314** (1987) 234.

[58] J. R. Ipser and L. Lindblom, Phys. Rev. Lett. **62** (1989) 2777.

[59] J. R. Ipser and L. Lindblom, Astrophys. J. **355** (1990) 226.

[60] R. A. Managan, Astrophys. J. **309** (1986) 598.

[61] E. Flowers and N. Itoh, Astrophys. J. **206** (1976) 218.

[62] R. F. Sawyer, Phys. Lett. **233** (1989) 412.

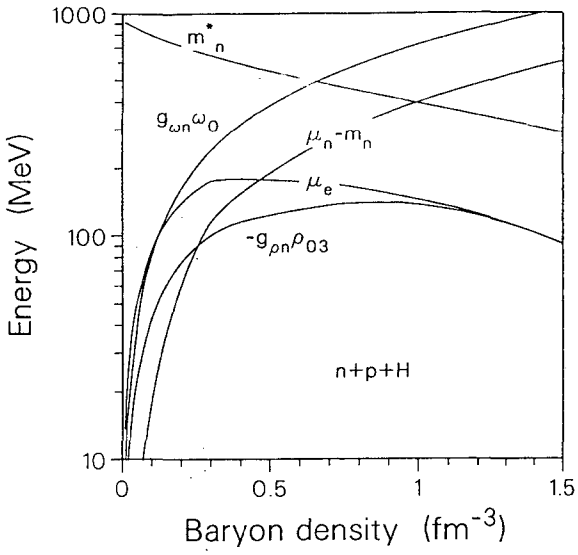

Figure 1: Field amplitudes and chemical potentials that solve eqs. (5-12) in the case of full equilibrium among all baryons to convergence. Baryons are coupled with $x = \sqrt{2/3}$. The Fermi momenta that constitute the rest of the solution are represented by the populations in Fig. 2.

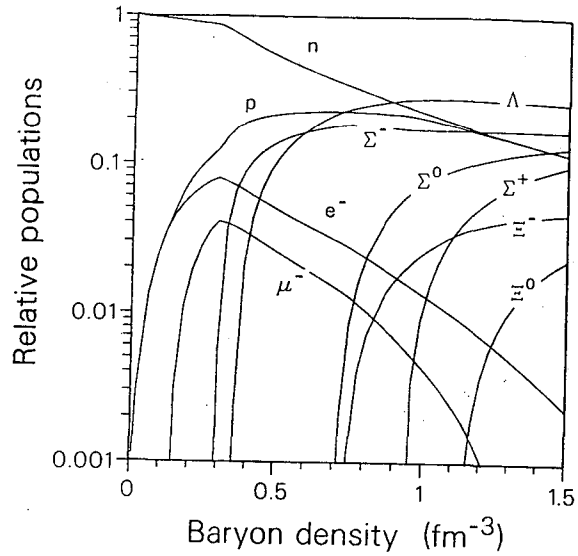

Figure 2: Populations in neutron star matter as a function of density for hyperon coupling $x = \sqrt{2/3}$.

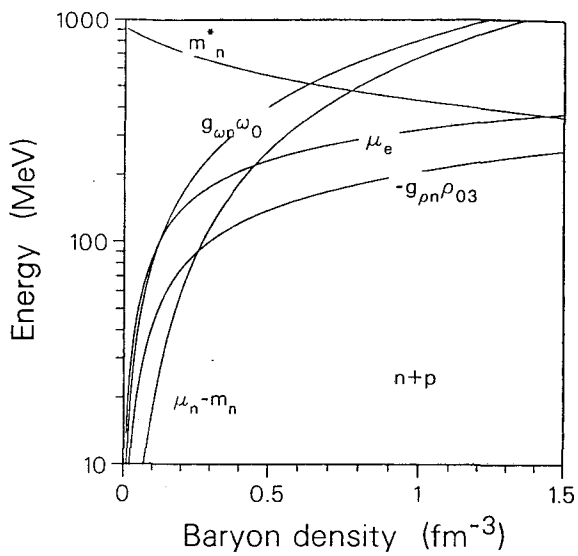

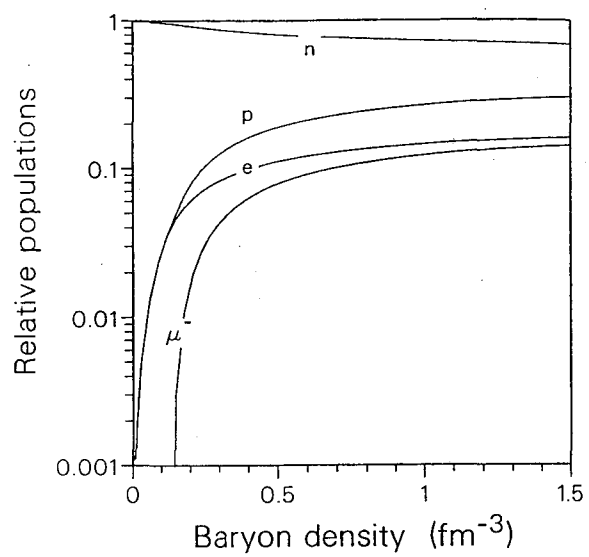

Figure 3: Similar to Figs. 1 and 2 but equilibrium involves only nucleons and leptons, with all higher baryon species omitted.

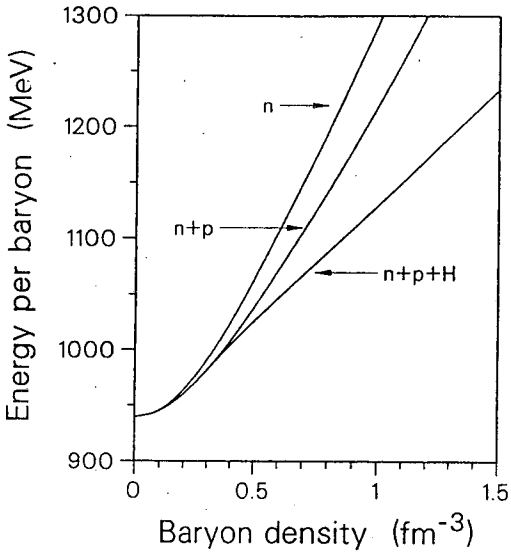

Figure 4: Equation of state for three cases; n - only neutrons; n+p - nucleons in beta equilibrium with leptons; and n+p+H - nucleons and all other baryons to convergence, with hyperons coupled with $x = \sqrt{2/3}$ and all in equilibrium with leptons.

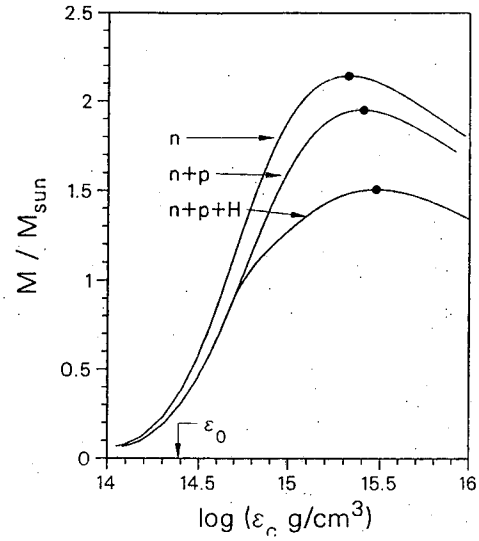

Figure 5: Star families for the three cases of Fig. 4. Density of normal nuclear matter is denoted by ϵ_0.

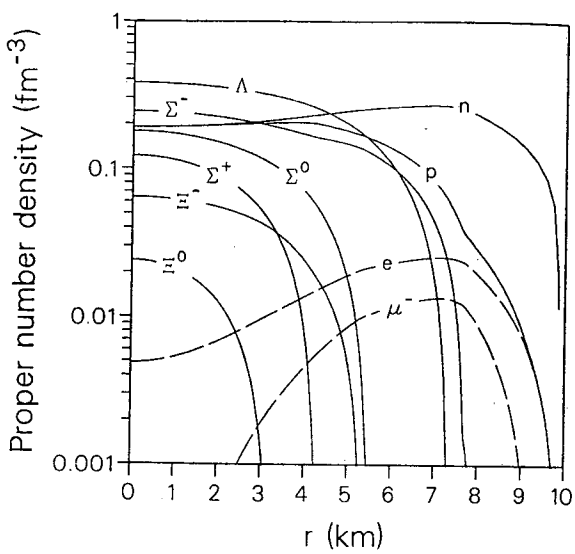

Figure 6: Populations in the maximum mass star corresponding to n+p+H in Fig. 5. Central baryon density is 1.4 fm^{-3}.

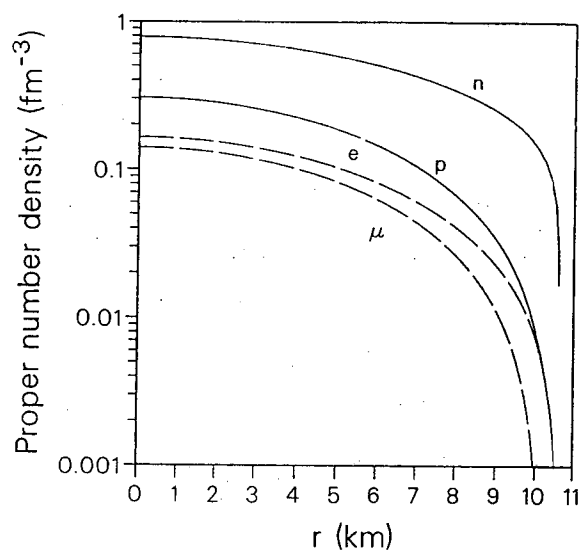

Figure 7: Populations in the maximum mass star corresponding to n+p in Fig. 5. Central baryon density is 1.1 fm^{-3}.

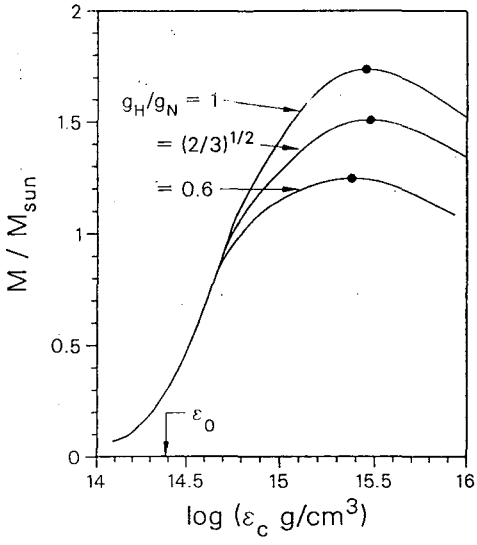

Figure 8: Neutron star families for three values of the hyperon to nucleon coupling constants.

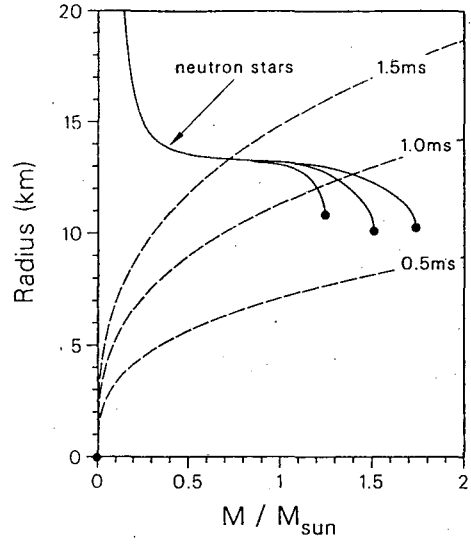

Figure 9: Mass-radius relation for the same star families as in Fig. 8.

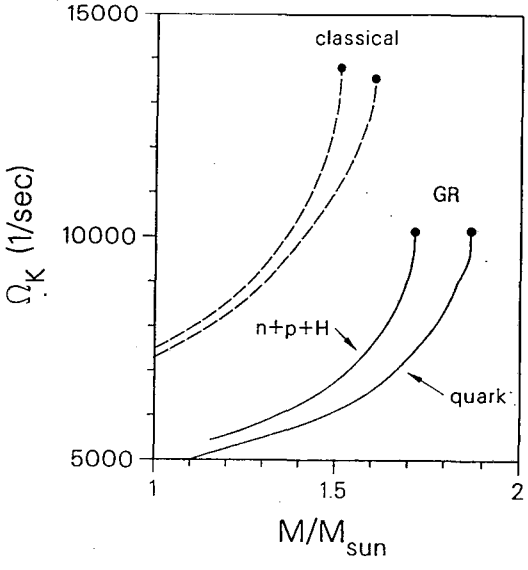

Figure 10: Kepler angular velocity in classical and general relativity physics for two sequences of stars, a 'neutron star', (n+p+H), and quark hybrid star.

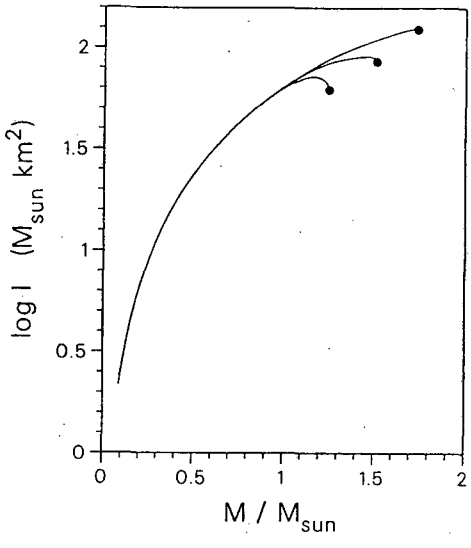

Figure 11: Moment of inertia for the same star families as in Fig. 8.

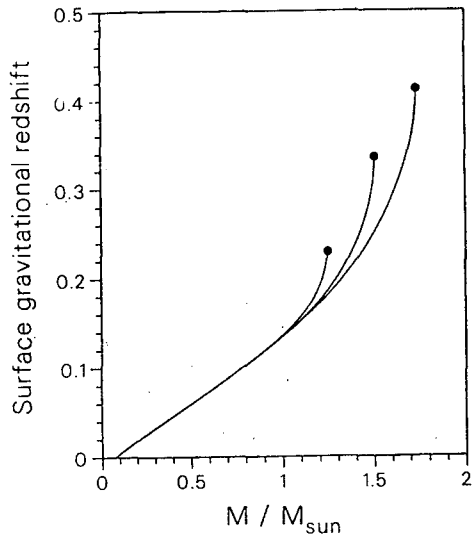

Figure 12: Surface redshift as a function of neutron star mass for the same families as in Fig. 8.

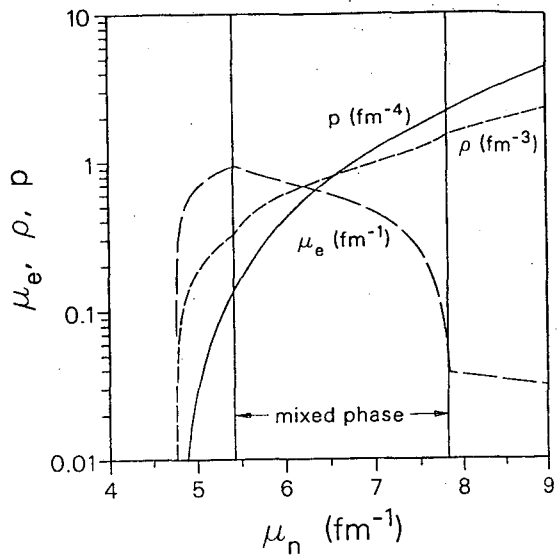

Figure 13: Showing finite width in neutron chemical potential of mixed phase with two conservation laws. Vertical lines denote boundaries separating mixed from the pure phases.

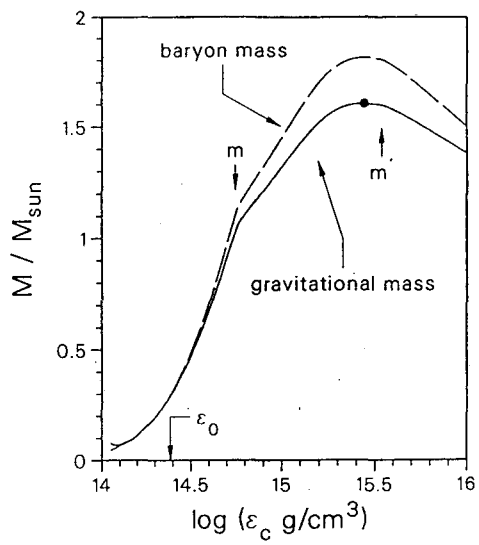

Figure 14: Family of stars in which the cores of the more massive ones (hybrids) is in the mixed phase of two components, confined and quark matter. Hyperons are coupled with $x = 1$.

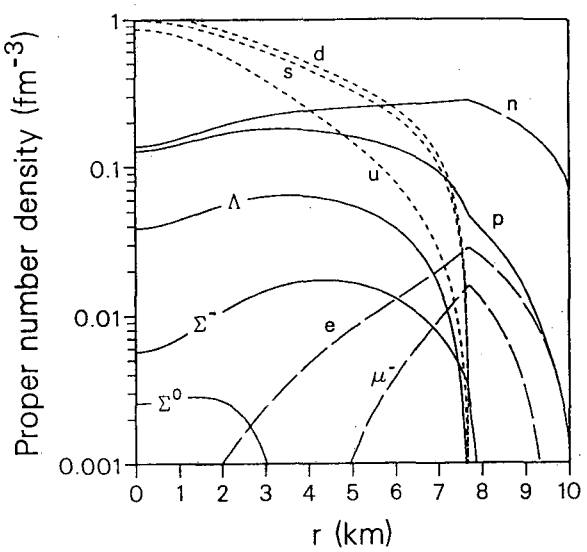

Figure 15: Populations of the most massive star of the family of hybrids of Fig. 14. Central baryon density is 1.3 fm^{-3}.

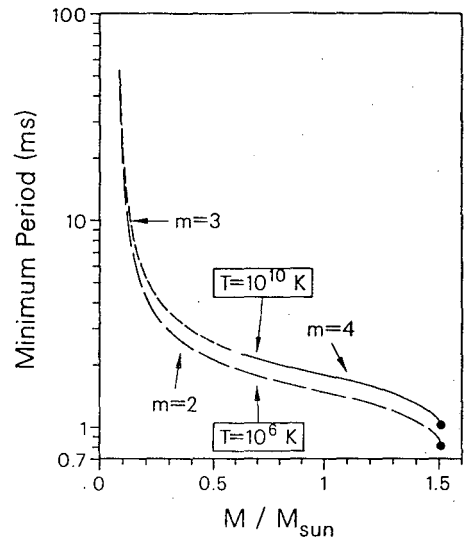

Figure 16: Minimum period that is stable against gravitational radiation-reaction for hot and cold stars for the family of neutron stars corresponding to the hyperon coupling $x = \sqrt{2/3}$ case of Fig. 8.

List of Figures

1 Field amplitudes and chemical potentials that solve eqs. (5 -12) in the case of full equilibrium among all baryons to convergence. Baryons are coupled with $x = \sqrt{2/3}$. The Fermi momenta that constitute the rest of the solution are represented by the populations in Fig. 2 24

2 Populations in neutron star matter as a function of density for hyperon coupling $x = \sqrt{2/3}$. 24

3 Similar to Figs. 1 and 2 but equilibrium involves only nucleons and leptons, with all higher baryon species omitted. 24

4 Equation of state for three cases; n - only neutrons; n+p - nucleons in beta equilibrium with leptons; and n+p+H - nucleons and all other baryons to convergence, with hyperons coupled with $x = \sqrt{2/3}$ and all in equilibrium with leptons. 25

5 Star families for the three cases of Fig. 4 . Density of normal nuclear matter is denoted by ϵ_0. 25

6 Populations in the maximum mass star corresponding to n+p+H in Fig. 5 . Central baryon density is 1.4 fm^{-3}. 25

7 Populations in the maximum mass star corresponding to n+p in Fig. 5 . Central baryon density is 1.1 fm^{-3}. 25

8 Neutron star families for three values of the hyperon to nucleon coupling constants. 26

9 Mass-radius relation for the same star families as in Fig. 8 26

10 Kepler angular velocity in classical and general relativity physics for two sequences of stars, a 'neutron star', (n+p+H), and quark hybrid star. 26

11 Moment of inertia for the same star families as in Fig. 8 26

12 Surface redshift as a function of neutron star mass for the same families as in Fig. 8 27

13 Showing finite width in neutron chemical potential of mixed phase with two conservation laws. Vertical lines denote boundaries separating mixed from the pure phases. 27

14 Family of stars in which the cores of the more massive ones (hybrids) is in the mixed phase of two components, confined and quark matter. Hyperons are coupled with $x = 1$. 27

15 Populations of the most massive star of the family of hybrids of Fig. 14 . Central baryon density is 1.3 fm^{-3}. 27

16 Minimum period that is stable against gravitational radiation-reaction for hot and cold stars for the family of neutron stars corresponding to the hyperon coupling $x = \sqrt{2/3}$ case of Fig. 8 28

List of Tables

1 Baryons and their charge states. Spin is J, isospin is I, its third component I_3, charge is q and strangeness is s. 6

2 Values of the hyperon to nucleon scalar and vector coupling that are compatible with the binding of −28 MeV for lambda hyperons in nuclear matter and the corresponding maximum neutron star mass. . . 10

LAWRENCE BERKELEY LABORATORY
UNIVERSITY OF CALIFORNIA
INFORMATION RESOURCES DEPARTMENT
BERKELEY, CALIFORNIA 94720